Internal polymeric coating materials for preventing pipeline hydrogen embrittlement and a theoretical model of hydrogen diffusion through coated steel

Y. Lei [a], E. Hosseini [a], L. Liu [b], C. A. Scholes [a], S.E. Kentish [a]*

[a] *Department of Chemical Engineering, The University of Melbourne, Vic, 3010, Australia*

[b] *CSIRO Mineral Resources, Pullenvale, Qld, 4069, Australia*

Abstract

This work develops a theoretical analysis of the coating permeability necessary for use as internal coatings of transmission pipelines to prevent hydrogen embrittlement. Internal coating materials suitable to be applied in situ on existing steel pipelines are also evaluated. Twelve different commercially available coatings; crosslinked poly (vinyl alcohol) (PVA), poly (vinyl chloride) and bisphenol A diglycidyl ether (DGEBA)/ polyetheramine (D-400) epoxy coatings prepared in-house were tested. Films fabricated from two commercial epoxies had hydrogen permeability of 0.40 Barrer and 0.35 Barrer respectively, which show potential as coating materials. A hydrogen permeability of 0.0084 Barrer was achieved with a crosslinked poly (vinyl alcohol) coating, indicating that this material shows the highest potential of all coatings tested. Unsteady-state hydrogen diffusion through coated steel was then modeled to evaluate the effect of the coating film in reducing hydrogen embrittlement. The result shows that with a 2mm PVA coating, hydrogen permeation inside the coating will take seven years to reach equilibrium and the final hydrogen concentration on the steel surface will be 44% lower than that without a coating. Greater protection can be provided if coatings can be developed with lower hydrogen permeability.

Key words: Hydrogen embrittlement; Hydrogen permeability; Poly vinyl alcohol; Polymer coatings; Steel pipeline

*Corresponding Author

1. Introduction

Hydrogen embrittlement (HE) is a generally recognized effect occurring in metals of high strength such as steel and has been a recognized problem for the hydrogen industry for decades.[1] There are a variety of mechanisms which can explain HE such as hydrogen enhanced decohesion (HEDE) and hydrogen enhanced local plasticity (HELP).[2–10] Pipeline steel failure resulting from hydrogen embrittlement usually initiates from defects and cracks on the pipe surface.[11] Hydrogen molecules dissociate into hydrogen atoms on this steel surface before entering the steel lattice. The atomic hydrogen dissolves into the steel and diffuses from the high-pressure to low-pressure side. [12,13] The dissolved hydrogen can degrade the mechanical properties of the steel pipes, for example, ductility, fracture toughness and fatigue life[14,15]. In order to transport hydrogen gas using steel pipelines, hydrogen embrittlement needs to be overcome.

In recent years, a number of methods to prevent hydrogen embrittlement on steel have been developed. These methods include cadmium and nickel plating[16], black oxide conversion coating[17,18], hard coatings such as TiO_2 to serve as barriers[19] and hydrogen trapping techniques[20,21].

Coating techniques generally reduce the rate of hydrogen transmission into the steel. This transmission can be described using a number of parameters i.e. the diffusivity, the permeability or the permeance. The units used to describe these parameters are summarized in the Supplementary Information (Table S1), for the convenience of the reader.

Studies have shown that coating with an appropriate metal or alloy can reduce the hydrogen penetration into steels.[1,16,21,22] Cadmium (Cd) has lower hydrogen diffusivity than common steels and is often used as a barrier for steels to prevent corrosion from the environment.[1] As with Cd, alloys of Nickel (Ni) also have low hydrogen diffusivity. The hydrogen diffusivity in Ni was determined to be 2.2×10^{-13} m^2/s at 25 ºC[23] while most steel has diffusivity around 10^{-10} m^2/s as presented in Table S2. [24–33] These metal and alloy coatings are deposited by electroplating. However, the process of electroplating itself can introduce hydrogen into steel and indeed it was found that Zn-Co alloy and Cd coatings have caused serious hydrogen embrittlement.[34] To mitigate against this effect, post heat treatment of the coated steels is necessary to allow hydrogen

to escape. Using a thermal immersion test with a constant heating rate, Ooi showed that a black oxide coating can resist hydrogen intake from decomposing lubricants used on steels.[17]

Hard nitrides, carbides and oxides such as TiO_2, TiC, Al_2O_3 and Cr_2O_3, are widely used in industry to provide protection of metal surfaces against chemical and mechanical attack.[35] They are also used in coatings for HE resistance due to their dense structures and low gas permeability. It was shown that even after hydrogen charging for 144h, the fracture toughness of a sample coated with CrN layers was sustained, while the fracture toughness of the control with no coating decreased by 66%.[36] Other studies shown that Al and Ti ceramic coatings can reduce hydrogen permeation by 1000 to 100,000 times.[37] These materials are generally coated using chemical or physical vapour deposition under vacuum conditions, so the possibility of embrittlement during these processes is low.[1,38] However, the performance of the coatings depends on the service conditions such as the defects on the metal surface and localized stress.[21] The coatings can be worn out or destroyed if the localized stresses are heavy.

Hydrogen can be trapped by non-ideal lattice structures in the steel such as grain boundaries and vacancies. These trapping sites can interfere with hydrogen diffusion and influence the HE process. It is difficult for hydrogen to diffuse through such disordered structures because to escape the trap, hydrogen needs to overcome a larger binding energy than the energy required to escape the normal lattice.[1,21,39] CHNS (carbon, hydrogen, nitrogen, and sulphur) elemental analysis has shown that these traps have a high hydrogen absorption capacity.[40] The presence of these irreversible traps can retard the hydrogen diffusion in steels and reduce hydrogen sensitivity[41]. There are different methods to introduce traps on the metal surface. Coatings can be obtained by deposition of niobium and cobalt using a high velocity oxygen fuel (HVOF) thermal spray.[20,40] Brandolt obtained a niobium (Nb) coating on standard steels which showed a 7.5 times higher hydrogen trapping capacity than that of the steel.[20] Traps can also be introduced by introducing damage to the metal surface via low energy implantation of helium and ion irradiation.[42]

Hydrogen barriers that use polymeric materials together with nanomaterials have also been investigated. Yang successfully fabricated polymer multilayer thin films as a gas barrier. Ten bilayers of polyethyleneimine (PEI) and poly acrylic acid (PAA) produced a thin film using poly (ethylene terephthalate) (PET) as a support that could reduce the oxygen transmission rate by about 1700 times.[43] However, the film was very thin, with a thickness of 305nm and so would be

difficult to construct across the large surface areas within hydrogen pipeline infrastructure. Also, with ten bilayers, the fabrication process will be complex. PEI has also been used in layer-by-layer (LbL) assembly with graphene oxide (GO). Thin films as hydrogen barriers were produced via LbL self-assembly of a GO suspension (pH 3.5) and PEI solution (pH 12). The thin film with 10 bilayers of GO and PEI were able to reach hydrogen transmission rates below 150 $cm^3/(m^2.d.bar)$, which is 0.0023 Gas Processing Units (GPU).[44] Li[45] and Liu[46] also obtained gas barrier films by LbL self-assembly using PEI and modified GO.

For large scale infrastructure and particularly for piping that is buried underground, suitable polymeric coatings and their delivery methods are required, which the above-mentioned coatings cannot achieve. For such infrastructure, the coating materials must be readily applied as near-ambient temperature solutions. Secondly, only very limited heating or other chemical treatments can be used to cure the coating. Finally, due to the very large areas covered by such infrastructure, the method should be cost effective without the use of expensive materials.

Based on these limitations, polymer coatings could be a useful option to solve the problem of hydrogen embrittlement while transporting hydrogen via existing pipelines. Polymer materials are easy to process and cost-effective. They have been used in various applications including gas barriers and coatings.[47–49]

A good example of low permeance barrier films is in the food packaging industry, where oxygen and water vapor permeability must be minimized to maintain shelf life and freshness.[50] The films developed for this industry may be viable for reducing hydrogen permeability in metal embrittlement situations. The most common packaging materials used for this purpose include ethylene vinyl alcohol (EVOH), polyvinylidene chloride (PVDC), oriented Nylon 6 and PVA. Most of these materials are manufactured by extrusion or lamination. PVC films have a low oxygen permeability of 0.005 – 0.12 Barrer[51]. The polymer has good solubility in tetrahydrofuran (THF) and can be applied on steel pipes in THF solutions. PVC has been used as coatings for pipeline corrosion resistance. Olad and Nosrati used PVC blended with ZnO nanoparticles in a THF solution as such a coating[52]. PVC/silica composite coatings have also been applied to two different steel substrates, showing good corrosion resistance[53].

Among these materials, PVA has very low oxygen permeability and it has good water solubility, which could provide a good coating option for hydrogen embrittlement. PVA coatings can be

fabricated by a solution casting method using water as the solvent. Crosslinked PVA films can lower gas permeability with a denser structure. Different crosslinking reagents have been explored, with results showing that glutaraldehyde is an effective reagent which gives a less swollen product.[54]

Most coatings used in the pipeline industry however, are epoxies or polyurethanes. Two-part epoxy coatings are generally applied on pipelines to prevent corrosion with good adhesion ability and processability.[55] These coatings can often be cured at room temperature and applied via air-spraying with liquid epoxy resin as one part and an appropriate curing agent as the second part. Lange[56] investigated the oxygen barrier properties of diglycidyl ethers of bisphenol and butanediol based epoxy coating films using different amines as the hardener. The results showed that aliphatic amines had the best gas barrier properties. A number of workers have already recorded the permeability of gases in these resins both with and without fillers to reduce gas permeation (Table S3). However, none to date have recorded the hydrogen permeability.

There are no clear indications in the literature as to what concentration of hydrogen inside the steel will cause embrittlement, as the type of steel, its working history and the specific location and size of defects all play a role. Rather, the permeability reduction factor (PRF) is usually used to show the quality of any coating in reducing embrittlement, defined as the steady-state ratio of the permeation rate through the uncoated steel J_s versus the permeation rate through the coated steel J_{coated}.[57]

$$PRF = \frac{J_S}{J_{coated}} \qquad (1)$$

Here, we first aim to identify the coating permeability that is required to provide a PRF of 10 at the hydrogen pressures that might be experienced in transmission pipelines. We then test a range of both commercially available and in-house prepared coating materials to determine their permeability and diffusivity. Based on these test results and related literature data, the unsteady-state hydrogen diffusion process through coated steel is modeled to evaluate the effectiveness of the coating layers identified to prevent embrittlement. The ultimate aim is to identify an internal coating for existing piping that provides a barrier to hydrogen permeation. The coating should be able to be applied in-situ, have low hydrogen permeability and be cost-effective.

2. Theory and Model Development

Hydrogen molecules dissociate into hydrogen atoms on a steel surface and diffuse through the steel as singular atoms [12]. These hydrogen atoms will first fill defects and the spaces between the grains within the steel, known as hydrogen traps. The initial diffusion coefficient (defined by the apparent diffusion coefficient, D_s) is low as these traps are filled. After extended exposure, these traps are filled and the diffusion coefficient increases to a steady state value (the lattice diffusion coefficient, D_L) [30]. The relationship between these two coefficient can be expressed by[27]:

$$D_s = \frac{D_L}{1+KN_T/N_L} \qquad (2)$$

K: Equilibrium constant;

N_L: The number of hydrogen atoms in lattice sites;

N_T: The number of hydrogen atoms in traps.

According to Sievert's law, the total concentration of the hydrogen atoms in steel (c_s) can be expressed by[28]:

$$c_s = S_s \sqrt{p} \qquad (3)$$

Where S_S is the solubility of hydrogen atoms in the steel, and p is the partial pressure of hydrogen molecules at the measurement point.

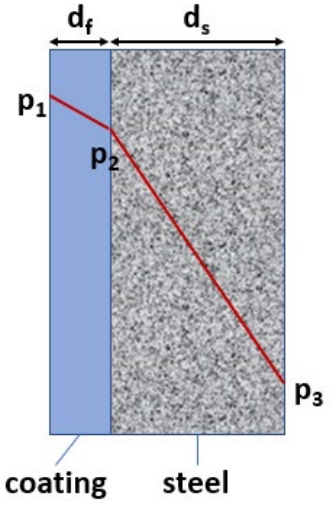

Figure 1 Schematic of the hydrogen concentration profile during permeation through a polymer coated steel specimen

The flux of hydrogen (J_s in mol H/m^2.s) through the steel specimen can then be determined by Fick's law (Equation 4)

$$J_s = D_s \frac{dC_s}{dx} = D_S S_S \frac{\sqrt{p_2} - \sqrt{p_3}}{d_s} \qquad (4)$$

where d_s is the thickness of the steel specimen, p_2 and p_3 are the partial pressure of hydrogen on the high and low pressure sides of the steel specimen (Figure 1).

The permeability of hydrogen through steel can be expressed by:

$$P_s = D_s . S_s \qquad (5)$$

There are two generally adopted methods to determine the hydrogen permeability of steel. In the gaseous method, hydrogen diffusivity and solubility of steel sample is measured at high temperature (>200 ºC) then the data are extrapolated to ambient temperature[24,25,28]. In the electrochemical method a Devanathan-Stachurski type two-component electrolytic permeation cell is used.[58,59] A range of hydrogen transport properties are reported in the Supplementary Information based on the two test types and it is readily apparent that the two methods produce widely different results. In particular, the gaseous method generally provides lower values of the apparent diffusion coefficient and higher values of the total solubility. This leads to values for the permeability that can be three orders of magnitude lower than that recorded using the electrochemical method (from 3.7 x 10^{-11} to 1.8 x 10^{-14} mol H /m.s.Pa$^{1/2}$). Conversely, the difference between the lattice diffusion coefficient and the apparent diffusion coefficient is much smaller for the electrochemical technique. This probably reflects the more unsteady state nature of the gaseous test method. In electrochemical methods, the steel is often pre-charged with hydrogen to approach steady state, whereas in gaseous testing this is not the case. Further, in the electrochemical method, hydrogen atoms can be produced and absorbed on steel surface directly by the electrochemical discharge of water molecules, while for the gaseous method, the hydrogen molecules need to dissociate into atoms first [60,61]. The different steel types used for testing and the work history of the steel can also influence the coefficients.

The hydrogen concentration in polymer film (c_f) can be expressed by:

$$c_f = S_f \cdot p \qquad (6)$$

where S_f (mol/m^3.Pa) is the solubility coefficient of hydrogen through the coating films.

Hydrogen permeates through polymer coatings in the form of hydrogen molecules. The flux of hydrogen through the film (J_f) in mol/m^2.s then can be given by:

$$J_f = D_f S_f \frac{(p_1 - p_2)}{d_f} = P_f \frac{(p_1 - p_2)}{d_f} \qquad (7)$$

where D_f (m^2/s) is the diffusivity coefficient of hydrogen through the coating films, P_f (mol.m^2/m^3.s.Pa) is the hydrogen permeability of coating films and d_f is the thickness of the film shown in Figure 1. This value is intrinsic to the material. The permeance determines the flux of hydrogen per unit pressure driving force, taking into account the sample thickness (Equation 8)

$$Permeance = \frac{P_f}{d_f} = \frac{J_f}{p_1 - p_2} \qquad (8)$$

The flux of hydrogen across the coating film and the steel should be identical for one coated steel specimen. The flux of atoms will be double the flux of molecules giving hydrogen is diatomic molecule.

$$J_S = 2J_f \qquad (9)$$

As an initial estimate, calculations were completed using Equations 1-9 for an internal pipe pressure of p_1= 10,000kPa and a wall thickness of 10mm, as estimates typical for transmission pipelines. It is assumed that the coating thickness is 1mm and hydrogen partial pressure at the external side of steel pipe is 0 (p_3=0). A tenfold reduction in flux (*PRF*=10) corresponds to a 100-fold reduction in the hydrogen pressure at the pipeline surface (p_2), due to the nature of Equation 4.

Table 1 An initial estimate of the required permeability of a 1mm coating to reduce hydrogen flux through a transmission pipeline operating at 10,000kPa internal pressure and with a wall thickness of 10mm

Pressure at pipe surface (kPa)	**Required coating permeability (Barrer)**	
	Steel hydrogen permeability = 3.7 x 10^{-11} mol H /m.s.$Pa^{1/2}$	**Steel hydrogen permeability = 1.8 x 10^{-14} mol H /m.s.$Pa^{1/2}$**
10,000	0.18	0.000086

From the calculation result, the hydrogen permeability of the coating required to reduce the hydrogen flux through a pipeline by 10-fold can vary from 0.000086 Barrer to 0.18 Barrer based on the full range of permeability values described in the Supplementary Information. This initial calculated result serves as a benchmark in terms of coating performance. The coating hydrogen permeability should be lower than 0.18 Barrer to provide any significant protection against hydrogen embrittlement.

However, these calculations are based on steady-state hydrogen diffusion through the coated steel. The coating can provide much better protection if the hydrogen diffusion process takes more time (of the order of years) to reach an equilibrium state. Non-steady state hydrogen diffusion through coated steel can be modeled using Fick's second law (Equation 10).[62]

$$D\frac{\partial^2 c}{\partial z^2} = \frac{\partial c}{\partial t} \qquad (10)$$

where c (mol/m^3) is the hydrogen concentration (hydrogen molecules in polymer coating and hydrogen atoms in steel); z (m) is the distance from the coating surface or steel surface to the measurement point; and t (s) is time.

In the present case, this unsteady-state hydrogen diffusion through uncoated steel and coated steel was modeled using MATLAB. Explicit discretization was used to solve Equation 10 as below.

$$\frac{c_z^{t+dt} - c_z^t}{dt} = D \cdot \frac{c_{z-dz}^t - 2c_z^t + c_{z+dz}^t}{(dz)^2} \qquad (11)$$

Rearranging equation 11:

$$c_z^{t+dt} = c_z^t + D \cdot \frac{dt}{(dz)^2}(c_{z-dz}^t - 2c_z^t + c_{z+dz}^t) \qquad (12)$$

Based on the discussion above, the initial and boundary conditions are:

$$c(t = 0) = 0 \quad (13)$$

$$c_f(t, z_f = 0) = p_1 S_f \quad (14)$$

$$c_s(t, z_s = d_s) = 0 \quad (15)$$

The modeling assumes that

a. The polymer coating and the steel are homogeneous.
b. The coating and steel thickness are much smaller than other dimensions, so the diffusion is only considered as a one-dimensional linear process.
c. The sorption of hydrogen onto the coating surface and hydrogen dissociation into the steel surface are much faster than the diffusion process, so hydrogen diffusion is the rate determining step.
d. The hydrogen diffusivity is constant and independent with time.

Equations 3 and 6 are used to determine the concentration of hydrogen at the boundaries of the steel and coating; while Equation 9 is used to indicate that at the interface between the coating and the steel, the hydrogen atom flux into the steel is doubled the hydrogen molecules flux from the coating film.

Based on the literature data provided in the Supplementary Information, it is assumed that the steady state hydrogen diffusivity in steel is 1×10^{-10} m^2/s and its permeability is 1×10^{-13} mol $H.m^{-1}.s^{-1}.Pa^{-1/2}$. The polymer coating and steel thickness are assumed to be 1mm and 1cm respectively. As above, it is assumed that pipeline operation pressure p_1 is 10,000 kPa and the hydrogen pressure on the external side of pipeline is 0.

3. Experimental

3.1 Materials

Poly vinyl alcohol (PVA, 89-98 kDa, 99+% hydrolyzed) was purchased from Sigma (St. Louis, USA). The crosslinking reagent glutaric dialdehyde (25%), was purchased from Merck Pty Ltd (Darmstadt, Germany). Hydrochloric acid (HCl) solution (32%) was purchased form UNIVAR (Victoria, Australia). Poly vinyl chloride (PVC) was purchased from Sigma (St. Louis, USA). Tetrahydrofuran (THF) was purchased from Chem-Supply (SA, Australia) Bisphenol A diglycidyl

ether (DGEBA) was purchased from Sigma (St. Louis, USA). Polyetheramine (D-400) was from Huntsman (Jeffamine® D-400, Texas, USA). Gas cylinders of H_2 (99.99% purity) was supplied by Coregas Pty Ltd.

Commercial coatings were provided by different suppliers under confidentiality agreements. Some coatings were provided as two- or three-part raw materials and free-standing films were then prepared in our laboratory, as described below. Other coatings were provided as cured films directly and were tested without further treatment.

3.2 Preparation of Films

To prepare 5 wt% PVA aqueous solutions, deionized water was added to a round bottom flask. The flask was placed in a water bath at 90 ºC and the liquid was stirred using a magnetic stir under reflux. During stirring, PVA powder was added into the flask. The mixture was stirred at 90 ºC for 2 h until the solution was clear and PVA was completely dissolved. The solution was transferred into a glass bottle and left still overnight to eliminate gas bubbles.

PVA films and glutaraldehyde crosslinked PVA films were fabricated by a solvent casting method. The PVA solution was mixed with glutaraldehyde. The PVA/GA monomer molar ratio was 0.02. 32% HCl solution was added as the catalyst, with an HCl/PVA monomer molar ratio of 0.05.[63] The mixed solution and pure PVA solution were cast onto glass petri dishes and left to dry at ambient conditions to simulate pipeline coating conditions. The thickness of fabricated films was 34±7μm. Film thickness was measured by a micrometer (Mitutoyo, Japan) with an accuracy of ± 1μm and was an average thickness of 10 locations on the film.

PVC films were prepared by a solvent casting method. 75mg/mL PVC was dissolved in tetrahydrofuran (THF, 98%) and cast on a petri dish which was left 2-3 days at ambient temperature. The thickness of fabricated films was 50-70 μm.

Epoxy films were prepared by mixing DGEBA and D400 in a stochiometric ratio. The mixture was cast on a cellophane sheet using a casting knife and left to dry in room temperature for 7 days. The films were 733±10 μm.

Commercially available coatings were made by mixing the relevant parts immediately prior to coating in the weight or volume ratio recommended by suppliers. After mixing, the wet mixture

was applied to a cellophane sheet and a casting knife was used to create a thin film. The film was left to dry at room temperature without further thermal treatment in order to simulate on-site pipeline coating conditions. The thickness of films fabricated in our laboratory was in the range of 100-200 µm while the cured films provided by suppliers are around 400-1300 µm. In total, 12 commercial coatings were tested for permeability, numbered from 1 to 12.

3.3 Single gas permeation measurement

The pure gas permeability of coated supports and free-standing films for different gases was tested using a constant volume/variable pressure apparatus at 35±0.1ºC.[64], as shown in Figure 2 The volume of the permeate piping was determined by calibration with commercial Styrex polystyrene film (Mitsubishi Plastics, Japan) with a known oxygen permeability of 2.27 Barrer at 30ºC and 1atm feed pressure.

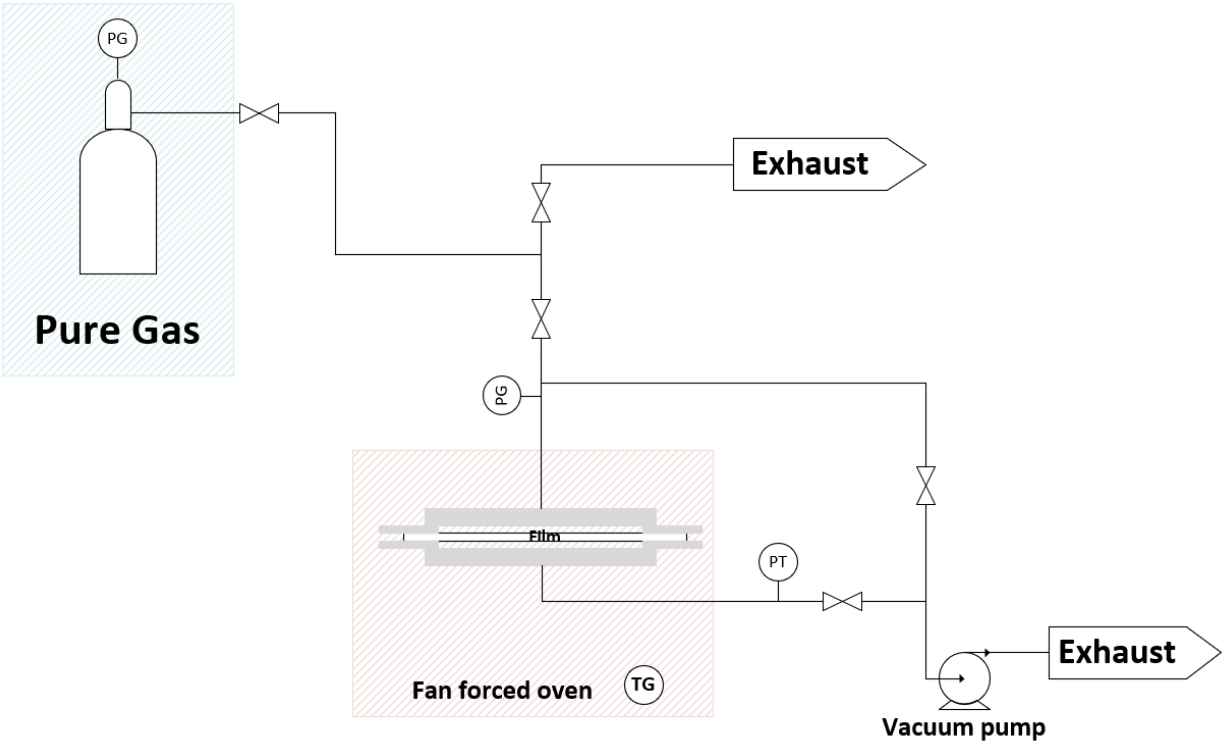

Figure 2 Pure gas permeation measurement apparatus

The film was placed in the holder which was placed in an oven to control the temperature. The system was connected to a vacuum pump. Before measurement, the film holder, the gas inlet and outlet tubing were placed under vacuum overnight to remove all gases. To measure the leakage rate of the apparatus, both the inlet and outlet valves of the gas tubing were closed and the pressure on the permeate side recorded by a pressure transducer (Baratron®, MKS, USA). To measure gas permeability, the pure gas feed was adjusted to the desired pressure and the gas inlet valve was opened. The permeate gas accumulated in the downstream piping and the pressure was recorded to calculate the gas permeability by equation 16 below.

$$P = \frac{273.2\times10^{10}}{760} \times \frac{lV}{AT\frac{p\times76}{14.7}} \times \left[\left(\frac{dp}{dt}\right) - \left(\frac{dp}{dt}\right)_{leakage}\right] \qquad (16)$$

P : gas permeability (Barrer, 10^{-10}cm^3(STP).cm.cm^{-2}.s^{-1}.cmHg^{-1});

l: film thickness (cm);

V: calibrated volume of downstream piping (cm^3);

A: film effective area (cm^2);

T: temperature of downstream piping (K);

p : absolute pressure of feed gas (psia);

$\frac{dp}{dt}$: pressure change with time in the permeate side (mmHg/s).

The gas diffusivity was obtained using the time-lag method, which utilises the unsteady state period at the beginning of the permeation period. The time-lag τ is defined as the intercept on the time-axis when the steady state linear relationship between downstream pressure and time is extrapolated backwards. The gas diffusivity D (m^2/s) can then be obtained by equation 3 below[65].

$$D = \frac{l^2}{6\tau} \qquad (17)$$

4. Results

4.1 Permeability and diffusivity of tested materials

The thickness, density, hydrogen permeability and diffusivity of different coating materials tested are illustrated in Table 2 and Figure 3.

Table 2 Film thickness, density, hydrogen permeability and diffusivity results of tested materials

		Type	Thickness (μm)	H_2 Permeability (Barrer)	H_2 Diffusivity (x 10^8 cm^2/s)	H_2 solubility ($mol/m^3.Pa$)	Density (g/cm^3)
Commercial coating	1	epoxy novolac	**292±8**	0.35±0.14	2.34±0.03	5.03E-05	2.11±0.003
	2	epoxy	**135±4**	0.40±0.02	84.0±14.2	1.61E-06	1.16±0.001
	3	epoxy novolac	**579±54**	0.64±0.01	17.6±0.8	1.22E-05	1.24±0.02
	4	epoxy	**441±11**	0.65±0.061			1.46±0.0004
	5	epoxy	**1284±40**	0.76±0.06	80.1±2.5	3.20E-06	1.34±0.004
	6	epoxy novolac	**517±9**	0.86±0.008	69.5±3.2	4.13E-06	1.55±0.002
	7	epoxy	**493±40**	0.97±0.01	10.3±0.3	3.16E-05	1.71±0.013
	8	epoxy	**193±14**	1.01±0.057	31.0±2.5	1.09E-05	1.58±0.002
	9	epoxy	**604±9**	1.21±0.015			1.62±0.05
	10	epoxy	**570±12**	1.21±0.09	70±1.0	5.79E-06	1.54±0.006
	11	polyurethane	**237±11**	1.98±0.11	138±7	4.82E-06	1.61±0.01
	12	polyurethane	**136±3**	18.1±1			
PVA			**33±9**	0.015±0.001	0.31±0.12	1.66E-05	1.25±0.031
PVA+GA			**36±5**	0.0084±0.0015	0.0147±0.0013	1.91E-04	1.27±0.004
PVC			**35±6**	2.44±0.003	294±38	2.78E-06	1.37±0.008
DGEBA+D400		epoxy	**733±10**	1.50±0.011	146±11	3.44E-06	1.16±0.002

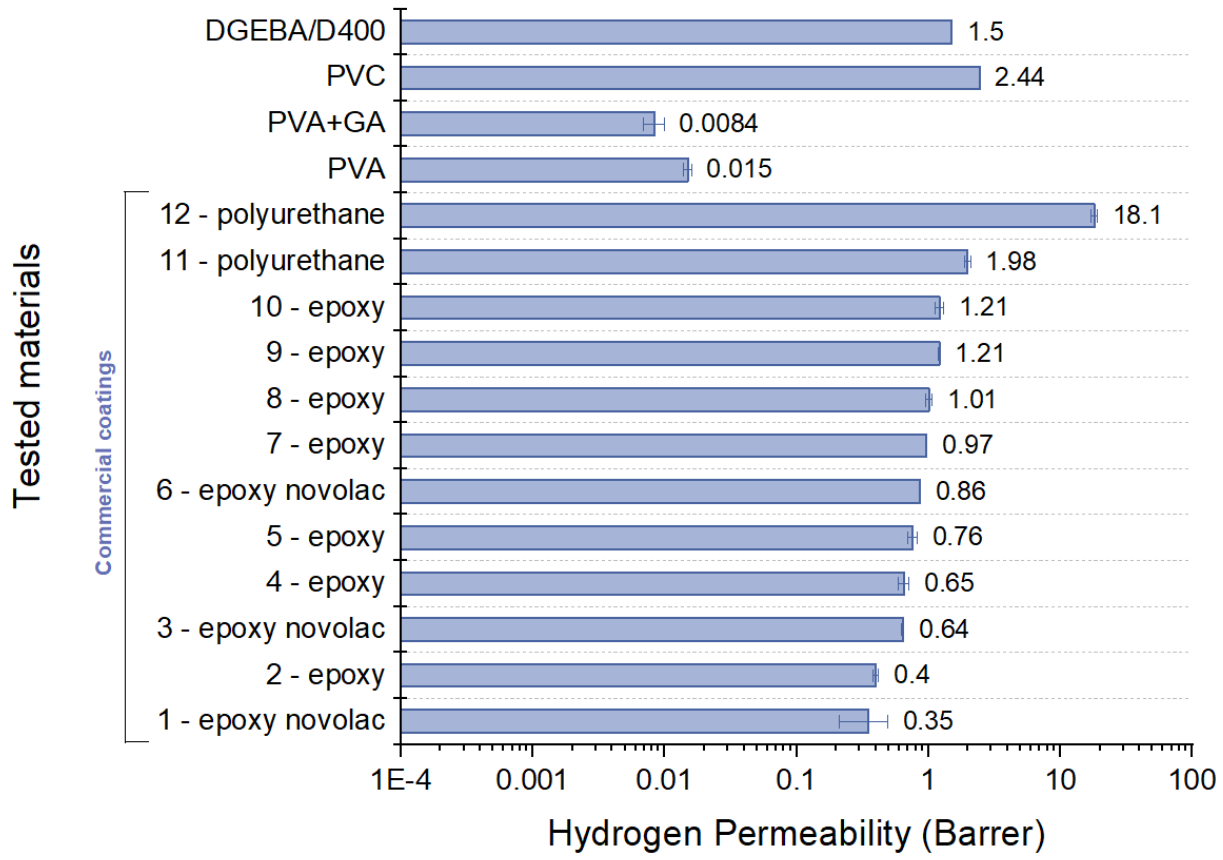

Figure 3 Hydrogen permeability of tested materials

It is apparent from Tables 1 and 2 that PVC and DGEBA/D400 coatings have hydrogen permeability which is too high to provide a significant resistance to hydrogen embrittlement (2.44 and 1.50 Barrer). PVA has a hydrogen permeability of 0.015 Barrer. The low permeability possibly results from the semi-crystalline structure of PVA.[66–68] PVA chains have many hydroxyl groups which can form inter and intra-molecular hydrogen bonds, resulting in folded and compacted regions which are impermeable to any penetrant [69,70] These crystalline regions increase the diffusion path of gas molecules and result in lower gas permeability.[71]

The glutaraldehyde crosslinked PVA provide values within the target range outlined in Table 1 with the lowest hydrogen permeability of 0.0084 Barrer. The hydroxy groups in PVA can react with aldehyde groups in glutaraldehyde under acidic environments[72], resulting in strong crosslinking. Hence crosslinked PVA shows great potential as the coating material.

Commercial epoxy coatings show better barrier properties than the polyurethane coatings tested in this work. Most commercially available coatings have hydrogen permeability below 1 Barrer. Among these coatings, there are two epoxy coatings having hydrogen permeability of 0.35 and 0.40 Barrer, which are close to the range of the initial estimates in Table 1, suggesting potential in internal coating materials to prevent hydrogen embrittlement on steel. However, these values are high compared to the permeability of PVA films. Further optimization could be done to provide a lower permeability to ensure that sufficient protection is provided for a range of pipelines.

The permeability and diffusivity results of crosslinked PVA coating was used for the unsteady state permeability modeling, given it has the lowest hydrogen permeability among all tested materials.

3.2 Unsteady State Modelling

Application of the unsteady state model described in Equations 10 to 15 shows that when diffusing through steel without a coating, the hydrogen concentration reaches an equilibrium after 8 days (Figure 2a), and the concentration on the steel internal surface is 3.16 mol/m^3. In Figure 2b Conversely, the diffusion process in an applied PVA coating takes two years to reach concentration equilibrium (Figure 2b). After 8 days, the hydrogen concentration on coated steel surface is only 0.0012 mol/m^3. After one year, the concentration on the coated steel surface reaches 1.9 mol/m^3, which is 40% lower compared than the uncoated steel surface. At equilibrium, the concentration on coated steel surface is 2.3 mol/m^3, 29% lower than that on uncoated steel surface. Hence, the time required to reach equilibrium is extended significantly with the PVA coating layer and the hydrogen concentration inside the steel is reduced, indicating the coating film has potential to prevent hydrogen embrittlement.

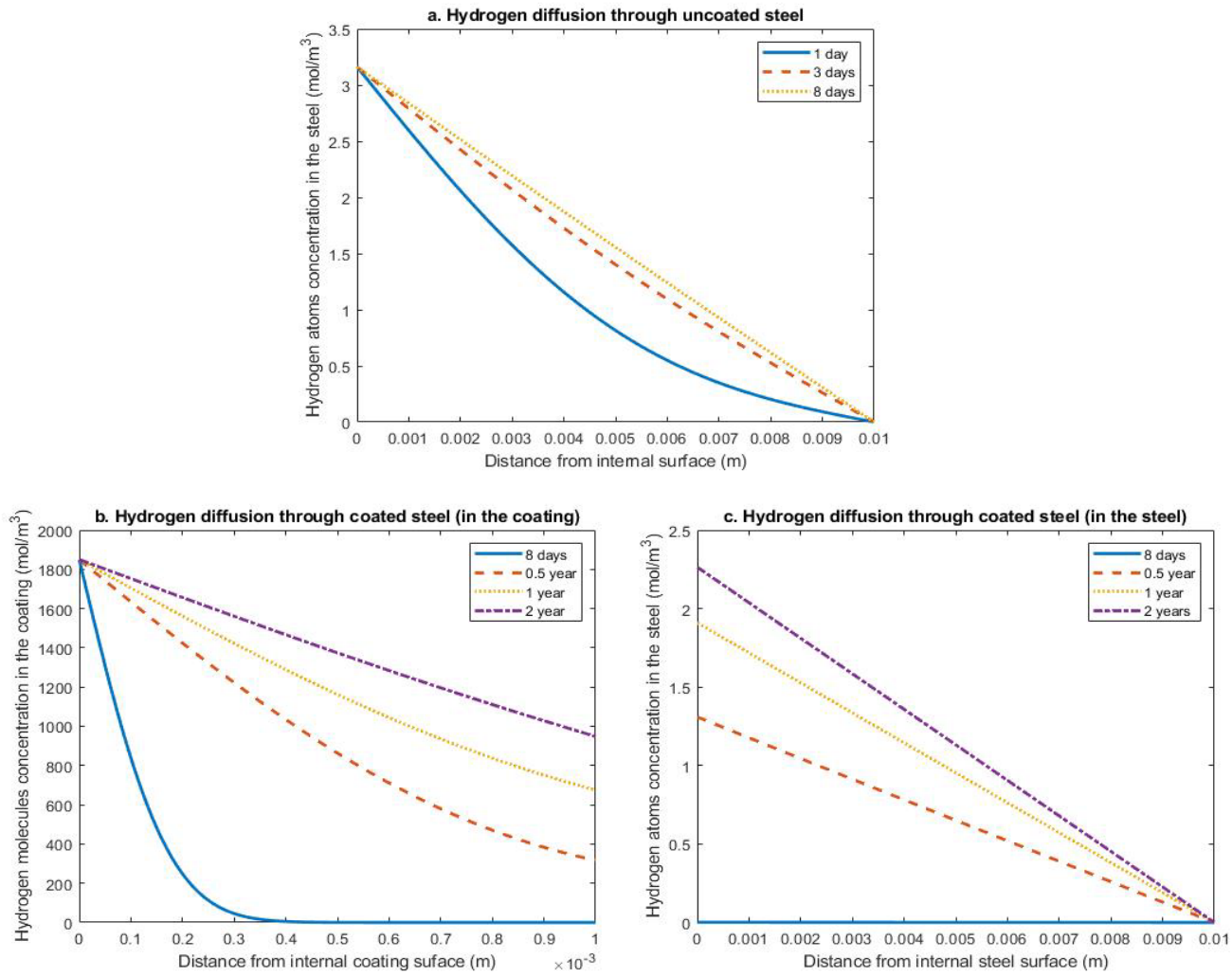

Figure 4 a. Hydrogen atom concentration distribution through steel without coating and concentration change with time (1 day, 3 days and 8 days); b. Hydrogen molecule concentration distribution throughout the coating (1mm) and concentration change with time (8 days, 0.5 year, 1 year and 2 years) in coated steel; c. Hydrogen atom concentration distribution throughout the steel and the concentration change with time (8 days, 0.5 year, 1 year and 2 years) in coated steel.

These results are influenced by the pipe wall thickness, the pipeline operating pressure, the hydrogen permeability of the steel, the coating permeability and the coating thickness. The first three factors depend on the actual pipeline working conditions. Conversely, the coating permeability depends on the material and the coating thickness, which can be controlled during application.

As one example, if the PVA coating thickness increases to 2 mm, the time to reach the concentration equilibrium will extend to seven years and the hydrogen concentration on the coated steel surface is 1.8 mol/m^3 (Figure 5) at equilibrium, a decrease of 44% compared with uncoated steel.

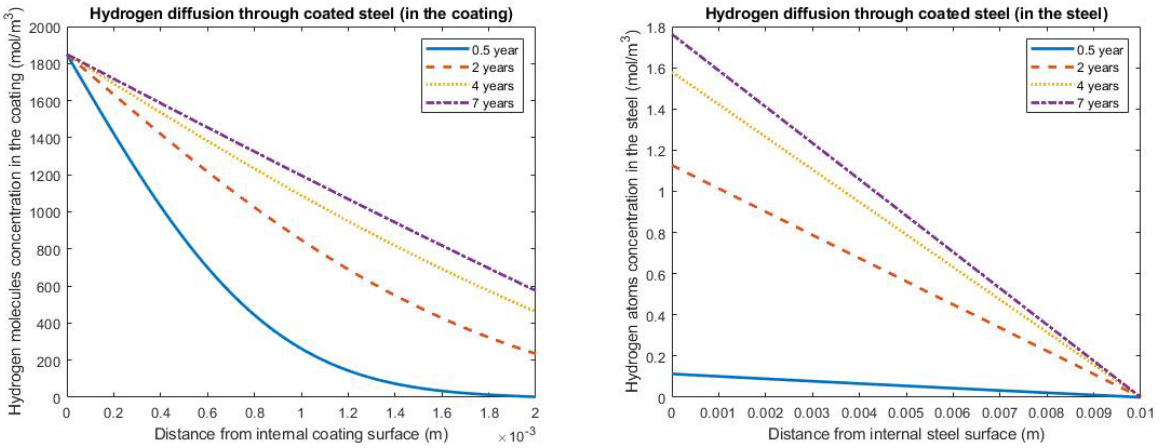

Figure 5 (a) Hydrogen molecule concentration distribution throughout the coating (2mm) and (b) atom concentration throughout the steel as a function of time (0.5 year, 2 years, 4 years and 7 years)

If the hydrogen permeability of the 1mm-thick coating can be reduced by 10-fold, with a 10-fold decrease in its hydrogen diffusivity, the time required to reach concentration equilibrium will extended to eight years as shown in Figure 6. The concentration inside steel at equilibrium can be reduced significantly with a hydrogen atom concentration of 0.49 mol/m^3 on steel surface, which is 85% lower than on the uncoated steel surface.

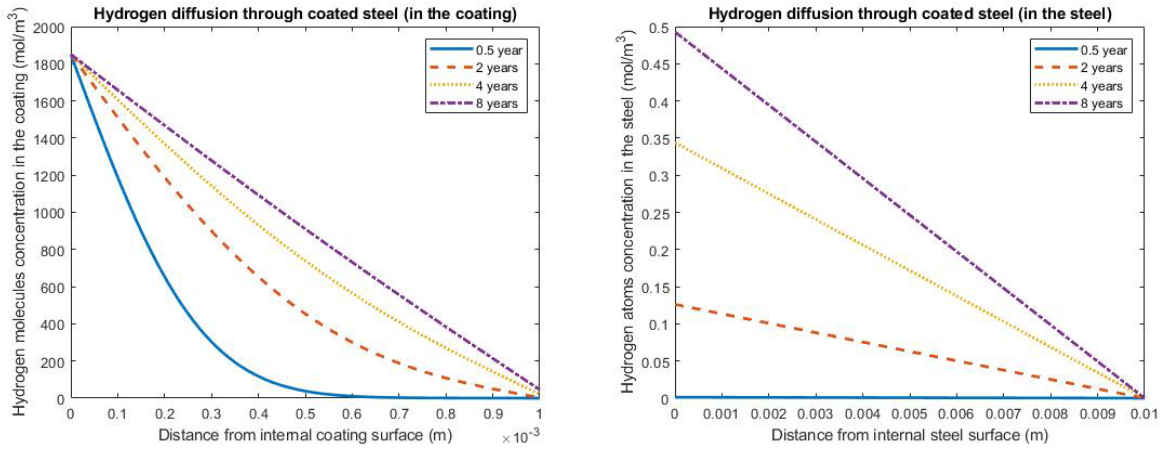

Figure 6 (a)Hydrogen molecule concentration distribution throughout the coating (1mm) with a 10-fold reduction in diffusivity and (b) atom concentration throughout the coated steel as a function of time (0.5 year, 2 years, 4 years and 7 years)

5. Conclusion

PVC, DGEBA/D400, PVA, crosslinked PVA films and twelve different commercial coatings have been prepared and tested for their hydrogen permeability and diffusivity. Films fabricated from two commercial epoxy resins have hydrogen permeability of 0.40 Barrer and 0.35 Barrer respectively, indicating potential as coating materials. However, the permeabilities are too high to act as a barrier material and therefore further modification is needed. Crosslinked PVA has a lowest hydrogen permeability of 0.0084 Barrer, indicating the strongest potential as the coating material.

Mathematical modeling of unsteady-state hydrogen diffusion through coated steel has been used to evaluate the influence of the crosslinked PVA coating upon hydrogen concentrations within the steel. The results demonstrate that a coating film with a thickness of 1 mm can extend the diffusion time to reach equilibrium to two years and substantially reduce the hydrogen concentration inside the steel. This result is influenced by the actual pipeline operation pressure, pipe wall thickness, the hydrogen permeability of the pipe steel itself and the coating thickness. If the thickness increases to 2 mm, the time to reach concentration equilibrium can be extended to seven years with a 44% reduction in the final hydrogen atom concentration on the steel surface. Further, if hydrogen diffusivity of the coating can be decreased by 10-fold, the time to reach equilibrium state will be extended to 8 years and the hydrogen concentration on the steel surface at equilibrium will decrease by 84%.

The impact of these changes in concentration on the hydrogen embrittlement process remain uncertain, as surveys of the literature provide little guidance as to the threshold hydrogen concentration that can lead to this condition. Determination of this concentration is outside the scope of the present paper but is of critical concern.

Acknowledgements

This work is funded by the Future Fuels CRC, supported through the Australian Government's Cooperative Research Centres Program. We gratefully acknowledge the cash and in-kind support from all the Future Fuels CRC's research, government and industry participants. The assistance provided by our Industry Advisory Team, particularly William Hughson from SEAGas, has been key to our understanding of these issues. We also acknowledge the suppliers who have provided us with coating materials, including AkzoNobel and Hempel.

References

[1] Dwivedi SK, Vishwakarma M. Hydrogen embrittlement in different materials: A review. Int J Hydrogen Energy 2018;43:21603–16. https://doi.org/10.1016/j.ijhydene.2018.09.201.

[2] Robertson IM, Sofronis P, Nagao A, Martin ML, Wang S, Gross DW, et al. Hydrogen Embrittlement Understood. Metall Mater Trans A 2015;46:2323–41. https://doi.org/10.1007/s11661-015-2836-1.

[3] Dear FF, Skinner GCG. Mechanisms of hydrogen embrittlement in steels: discussion. Philos Trans R Soc A Math Phys Eng Sci 2017;375:20170032. https://doi.org/10.1098/rsta.2017.0032.

[4] Gangloff RP. Hydrogen assisted cracking of high strength alloys. Compr Struct Integr 2003;6:31–101.

[5] Lynch SP. Hydrogen embrittlement (HE) phenomena and mechanisms. Stress Corros. Crack. Theory Pract., 2011, p. 90–130. https://doi.org/10.1533/9780857093769.1.90.

[6] Troiano AR. The Role of Hydrogen and Other Interstitials in the Mechanical Behavior of Metals. Metallogr Microstruct Anal 2016;5:557–69. https://doi.org/10.1007/s13632-016-0319-4.

[7] Ramamurthy S, Atrens A. Stress corrosion cracking of high-strength steels. Corros Rev 2013;31:1–31. https://doi.org/10.1515/corrrev-2012-0018.

[8] Hooshmand Zaferani S, Miresmaeili R, Pourcharmi MK. Mechanistic models for environmentally-assisted cracking in sour service. Eng Fail Anal 2017;79:672–703.

https://doi.org/10.1016/j.engfailanal.2017.05.005.

[9] Beachem CD. A new model for hydrogen-assisted cracking (hydrogen “embrittlement”). Metall Trans 1972;3:441–55. https://doi.org/10.1007/BF02642048.

[10] Kappes M, Iannuzzi M, Carranza RM. Hydrogen embrittlement of Magnesium and Magnesium Alloys: A review. J Electrochem Soc 2013;160:168–78. https://doi.org/10.1149/2.023304jes.

[11] Elazzizi A, Hadj Meliani M, Khelil A, Pluvinage G, Matvienko YG. The master failure curve of pipe steels and crack paths in connection with hydrogen embrittlement. Int J Hydrogen Energy 2015;40:2295–302. https://doi.org/10.1016/j.ijhydene.2014.12.040.

[12] Falco MD De, Marrelli L, Iaquaniello G. Membrane Reactors for Hydrogen Production Processes. vol. 66. London: Springer London; 2011. https://doi.org/10.1007/978-0-85729-151-6.

[13] Tamura M, Eguchi T. Nanostructured thin films for hydrogen-permeation barrier. J Vac Sci Technol A Vacuum, Surfaces, Film 2015;33:041503. https://doi.org/10.1116/1.4919736.

[14] Rajabipour A, Melchers RE. Service life of corrosion pitted pipes subject to fatigue loading and hydrogen embrittlement. Int J Hydrogen Energy 2018;43:8440–50. https://doi.org/10.1016/j.ijhydene.2018.03.063.

[15] Leeuwen HP Van. The kinetics of hydrogen embrittlement: A quantitative diffusion model. Eng Fract Mech 1974;6:141–61. https://doi.org/10.1016/0013-7944(74)90053-8.

[16] Shen S, Song X, Li Q, Li X, Zhu R, Yang G. Effect of Cr x C y –NiCr coating on the hydrogen embrittlement of 17-4 PH stainless steel using the smooth bar tensile test. J Mater Sci 2019;54:7356–68. https://doi.org/10.1007/s10853-019-03356-4.

[17] Ooi SW, Yan P, Vegter RH. Black oxide coating and its effectiveness on prevention of hydrogen uptake. Mater Sci Technol (United Kingdom) 2019;35:12–25. https://doi.org/10.1080/02670836.2018.1530425.

[18] Song RH, Pyun S Il, Oriani RA. The hydrogen permeation through passivating film on iron by modulation method. Electrochim Acta 1991;36:825–31. https://doi.org/10.1016/0013-4686(91)85280-K.

[19] Morimoto T, Kumai T. Prevention of Hydrogen Embrittlement Using Ultra Rapid Cooling Thermal Spraying Gun. ISIJ Int 2017;57:1461–7. https://doi.org/10.2355/isijinternational.isijint-2017-060.

[20] Brandolt C de S, Noronha LC, Hidalgo GEN, Takimi AS, Schroeder RM, Malfatti C de F. Niobium coating applied by HVOF as protection against hydrogen embrittlement of API 5CT P110 steel. Surf Coatings Technol 2017;322:10–8. https://doi.org/10.1016/j.surfcoat.2017.05.017.

[21] Bhadeshia HKDH. Prevention of Hydrogen Embrittlement in Steels. ISIJ Int 2016;56:24–36. https://doi.org/10.2355/isijinternational.isijint-2015-430.

[22] Kim H, Popov BN, Chen KS. Comparison of corrosion-resistance and hydrogen permeation properties of Zn-Ni, Zn-Ni-Cd and Cd coatings on low-carbon steel. Corros Sci 2003;45:1505–21. https://doi.org/10.1016/S0010-938X(02)00228-7.

[23] Hill ML, Johnson EW. The diffusivity of hydrogen in nickel. Acta Metall 1955;3:566–71. https://doi.org/10.1016/0001-6160(55)90116-4.

[24] Esteban GA, Perujo A, Douglas K, Sedano LA. Tritium diffusive transport parameters and trapping effects in the reduced activating martensitic steel OPTIFER-IVb. J Nucl Mater 2000;281:34–41. https://doi.org/10.1016/S0022-3115(00)00188-4.

[25] Forcey KS, Iordanova I, Ross DK. Investigation of structure dependence of diffusivity, solubility, and permeability of hydrogen in hot rolled low carbon steels. Mater Sci Technol (United Kingdom) 1990;6:357–63. https://doi.org/10.1179/mst.1990.6.4.357.

[26] Mohtadi-Bonab MA, Szpunar JA, Collins L, Stankievech R. Evaluation of hydrogen induced cracking behavior of API X70 pipeline steel at different heat treatments. Int J Hydrogen Energy 2014;39:6076–88. https://doi.org/10.1016/j.ijhydene.2014.01.138.

[27] Fallahmohammadi E, Bolzoni F, Lazzari L. Measurement of lattice and apparent diffusion coefficient of hydrogen in X65 and F22 pipeline steels. Int J Hydrogen Energy 2013;38:2531–43. https://doi.org/10.1016/j.ijhydene.2012.11.059.

[28] Bryan WL, Dodge BF. Diffusivity of hydrogen in pure iron. AIChE J 1963;9:223–8. https://doi.org/10.1002/aic.690090217.

[29] Serna S, Martínez H, López SY, González-Rodríguez JG, Albarrán JL. Electrochemical technique applied to evaluate the hydrogen permeability in microalloyed steels. Int J Hydrogen Energy 2005;30:1333–8. https://doi.org/10.1016/j.ijhydene.2005.04.012.

[30] Park GT, Koh SU, Jung HG, Kim KY. Effect of microstructure on the hydrogen trapping efficiency and hydrogen induced cracking of linepipe steel. Corros Sci 2008;50:1865–71. https://doi.org/10.1016/j.corsci.2008.03.007.

[31] Haq AJ, Muzaka K, Dunne DP, Calka A, Pereloma E V. Effect of microstructure and composition on hydrogen permeation in X70 pipeline steels. Int J Hydrogen Energy 2013;38:2544–56. https://doi.org/10.1016/j.ijhydene.2012.11.127.

[32] Dong CF, Li XG, Liu ZY, Zhang YR. Hydrogen-induced cracking and healing behaviour of X70 steel. J Alloys Compd 2009;484:966–72. https://doi.org/10.1016/j.jallcom.2009.05.085.

[33] Miller RF, Hudson JB, Ansell GS. Permeation of hydrogen through alpha iron. Metall Trans A 1975;6:117–21. https://doi.org/10.1007/BF02673678.

[34] Hillier EMK, Robinson MJ. Hydrogen embrittlement of high strength steel electroplated with zinc-cobalt alloys. Corros Sci 2004;46:715–27. https://doi.org/10.1016/S0010-938X(03)00180-X.

[35] Hintermann HE. Adhesion, friction and wear of thin hard coatings. Wear 1984;100:381–97. https://doi.org/10.1016/0043-1648(84)90023-1.

[36] Lee SC, Ho WY, Huang CC, Meletis EI, Liu Y. Hydrogen embrittlement and fracture toughness of a titanium alloy with surface modification by hard coatings. J Mater Eng Perform 1996;5:64–70. https://doi.org/10.1007/BF02647271.

[37] Hollenberg GW, Simonen EP, Kalinin G, Terlain A. Tritium/hydrogen barrier development. Fusion Eng Des 1995;28:190–208. https://doi.org/10.1016/0920-3796(95)90039-X.

[38] Kaestner P, Olfe J, He JW, Rie KT. Improvement in the load-bearing capacity and adhesion of TiC coatings on TiAl6V4 by duplex treatment. Surf Coatings Technol 2001;142–144:928–33. https://doi.org/10.1016/S0257-8972(01)01214-2.

[39] Liu MA, Rivera-Díaz-del-Castillo PEJ, Barraza-Fierro JI, Castaneda H, Srivastava A. Microstructural influence on hydrogen permeation and trapping in steels. Mater Des 2019;167:107605. https://doi.org/10.1016/j.matdes.2019.107605.

[40] Brandolt C de S, Malfatti C de F, Ortega Vega MR, Hidalgo GEN, Schroeder RM. Determination of hydrogen trapping mechanisms by microprinting in Ni and Co coatings obtained by HVOF. Surf Coatings Technol 2019;362:262–73. https://doi.org/10.1016/j.surfcoat.2019.01.111.

[41] Venezuela J, Zhou Q, Liu Q, Zhang M, Atrens A. Hydrogen Trapping in Some Automotive Martensitic Advanced High-Strength Steels. Adv Eng Mater 2018;20:1–14. https://doi.org/10.1002/adem.201700468.

[42] Xu Q, Zhang J. Novel Methods for Prevention of Hydrogen Embrittlement in Iron. Sci Rep 2017;7. https://doi.org/10.1038/s41598-017-17263-8.

[43] Yang YH, Haile M, Park YT, Malek FA, Grunlan JC. Super gas barrier of all-polymer multilayer thin films. Macromolecules 2011;44:1450–9. https://doi.org/10.1021/ma1026127.

[44] Zhao L, Zhang H, Kim NH, Hui D, Lee JH, Li Q, et al. Preparation of graphene oxide/polyethyleneimine layer-by-layer assembled film for enhanced hydrogen barrier property. Compos Part B Eng 2016;92:252–8. https://doi.org/10.1016/j.compositesb.2016.02.037.

[45] Li P, Chen K, Zhao L, Zhang H, Sun H, Yang X, et al. Preparation of modified graphene oxide/polyethyleneimine film with enhanced hydrogen barrier properties by reactive layer-by-layer self-assembly. Compos Part B Eng 2019;166:663–72. https://doi.org/10.1016/j.compositesb.2019.02.058.

[46] Liu H, Kuila T, Kim NH, Ku BC, Lee JH. In situ synthesis of the reduced graphene oxide-polyethyleneimine composite and its gas barrier properties. J Mater Chem A 2013;1:3739–46. https://doi.org/10.1039/c3ta01228j.

[47] Guan S, Mayes P, Andrenacci A, Wong D, Shawcor BS. Advanced Two Layer Polyethylene Coating Technology for Pipeline Protection 2007:1–7.

[48] Galić K, Kurek M, Ščetar M. Barrier Properties of Plastic Polymers. Ref. Modul. Food Sci., 2017. https://doi.org/10.1016/b978-0-08-100596-5.22369-x.

[49] McAndrew TP, Audenaert M, Petersheim J, Garcia D, Richards T. Polyamide-11 Powder Coatings: Exceptional Resistance to Cavitation Erosion, 2007, p. 190–200. https://doi.org/10.1021/bk-2007-0962.ch013.

[50] Bhunia K, Zhang H, Sablani SS. Gas Barrier Packaging. Ref. Modul. Food Sci., 2016. https://doi.org/10.1016/b978-0-08-100596-5.03219-4.

[51] Robertson GL. Food packaging: Principles and practice. 2013.

[52] Olad A, Nosrati R. Preparation and corrosion resistance of nanostructured PVC/ZnO-polyaniline hybrid coating. Prog Org Coatings 2013;76:113–8. https://doi.org/10.1016/j.porgcoat.2012.08.017.

[53] Conradi M, Kocijan A, Zorko M, Jerman I. Effect of silica/PVC composite coatings on steel-substrate corrosion protection. Prog Org Coatings 2012;75:392–7. https://doi.org/10.1016/j.porgcoat.2012.07.008.

[54] Bolto B, Tran T, Hoang M, Xie Z. Crosslinked poly(vinyl alcohol) membranes. Prog Polym Sci 2009;34:969–81. https://doi.org/10.1016/j.progpolymsci.2009.05.003.

[55] Wei R, Wang X, Zhang X, Chen C, Du S. Fabrication of high gas barrier epoxy nanocomposites: An approach based on layered silicate functionalized by a compatible and reactive modifier of epoxy-diamine adduct. Molecules 2018;23. https://doi.org/10.3390/molecules23051075.

[56] Lange J, Nicolas B, Galy J, Gerard JF. Influence of structure and chemical composition on oxygen permeability of crosslinked epoxy-amine coatings. Polymer (Guildf) 2002;43:5985–94. https://doi.org/10.1016/S0032-3861(02)00502-5.

[57] Nemanič V. Hydrogen permeation barriers: Basic requirements, materials selection, deposition methods, and quality evaluation. Nucl Mater Energy 2019;19:451–7. https://doi.org/10.1016/j.nme.2019.04.001.

[58] Devanathan MA V., Stachurski Z. The Mechanism of Hydrogen Evolution on Iron in Acid Solutions by Determination of Permeation Rates. J Electrochem Soc 1964;111:619. https://doi.org/10.1149/1.2426195.

[59] Devanathan M. A. V., Stachurski Z. The Adsorption and Diffusion of Electrolytic Hydrogen in Palladium. Proc R Soc London Ser A Math Phys Sci 1962;270:90–102.

[60] Bockris JOM, Subramanyan PK. The equivalent pressure of molecular hydrogen in cavities within metals in terms of the overpotential developed during the evolution of hydrogen. Electrochim Acta 1971;16:2169–79. https://doi.org/10.1016/0013-4686(71)85027-2.

[61] Liu Q, Atrens AD, Shi Z, Verbeken K, Atrens A. Determination of the hydrogen fugacity during electrolytic charging of steel. Corros Sci 2014;87:239–58. https://doi.org/10.1016/j.corsci.2014.06.033.

[62] Maiti, Bidinger. Polymer Permeability. vol. 53. Dordrecht: Springer Netherlands; 1985. https://doi.org/10.1007/978-94-009-4858-7.

[63] Dodda JM, Bělský P, Chmelař J, Remiš T, Smolná K, Tomáš M, et al. Comparative study of PVA/SiO2 and PVA/SiO2/glutaraldehyde (GA) nanocomposite membranes prepared by single-step solution casting method. J Mater Sci 2015;50:6477–90. https://doi.org/10.1007/s10853-015-9206-7.

[64] Kanehashi S, Nakagawa T, Nagai K, Duthie X, Kentish S, Stevens G. Effects of carbon dioxide-induced plasticization on the gas transport properties of glassy polyimide membranes. J Memb Sci 2007;298:147–55. https://doi.org/10.1016/j.memsci.2007.04.012.

[65] Michaels AS, Parker RB. Sorption and flow of gases in polyethylene. J Polym Sci 1959;41:53–71. https://doi.org/10.1002/pol.1959.1204113805.

[66] Cano AI, Cháfer M, Chiralt A, González-Martínez C. Physical and microstructural properties of biodegradable films based on pea starch and PVA. J Food Eng 2015;167:59–64. https://doi.org/10.1016/j.jfoodeng.2015.06.003.

[67] Nangia R, Shukla NK, Sharma A. Preparation, Structural and Dielectric Properties of Solution Grown Polyvinyl Alcohol(PVA) Film. IOP Conf Ser Mater Sci Eng 2017;225:012044. https://doi.org/10.1088/1757-899x/225/1/012044.

[68] El-Okazy MA, Liu L, Abdellah MH, Goudeli E, Kentish SE. Gas sorption and diffusion in perfluoro(butenyl vinyl ether) based perfluoropolymeric membranes. J Memb Sci 2022;644:120095. https://doi.org/10.1016/j.memsci.2021.120095.

[69] Assender HE, Windle AH. Crystallinity in poly(vinyl alcohol). 1. An X-ray diffraction study of atactic PVOH. Polymer (Guildf) 1998;39:4295–302. https://doi.org/10.1016/S0032-3861(97)10296-8.

[70] Amanda A, Kulprathipanja A, Toennesen M, Mallapragada SK. Semicrystalline poly(vinyl alcohol) ultrafiltration membranes for bioseparations. J Memb Sci 2000;176:87–95. https://doi.org/10.1016/S0376-7388(00)00433-6.

[71] Horas JA, Rizzotto MG. Gas diffusion in partially crystalline polymers part I: Concentration dependence. J Polym Sci Part B Polym Phys 1996;34:1541–6. https://doi.org/10.1002/(SICI)1099-0488(19960715)34:9<1541::AID-POLB2>3.0.CO;2-O.

[72] Rudra R, Kumar V, Kundu PP. Acid catalysed cross-linking of poly vinyl alcohol (PVA) by glutaraldehyde: effect of crosslink density on the characteristics of PVA membranes used in single chambered microbial fuel cells. RSC Adv 2015;5:83436–47. https://doi.org/10.1039/c5ra16068e.

Author/s:
Lei, Y;Hosseini, E;Liu, L;Scholes, CA;Kentish, SE

Title:
Internal polymeric coating materials for preventing pipeline hydrogen embrittlement and a theoretical model of hydrogen diffusion through coated steel

Date:
2022-08-26

Citation:
Lei, Y., Hosseini, E., Liu, L., Scholes, C. A. & Kentish, S. E. (2022). Internal polymeric coating materials for preventing pipeline hydrogen embrittlement and a theoretical model of hydrogen diffusion through coated steel. INTERNATIONAL JOURNAL OF HYDROGEN ENERGY, 47 (73), pp.31409-31419. https://doi.org/10.1016/j.ijhydene.2022.07.034.

Persistent Link:
http://hdl.handle.net/11343/324526